Decentralized Total Transfer Capability Evaluation Using Domain Decomposition Methods

Xiaochen Zhang, *Student Member, IEEE*, and Santiago Grijalva, *Senior Member, IEEE*

***Abstract*—In order to ensure the reliable operation of the electric power grid, infrastructure with increasing levels of distributed generation deployment, various entities and subsystems (e.g., ISOs, distribution utilities, micro-grids) needs a higher level coordination. Such coordination requires a formal decentralized control and management architecture that creates mechanisms for the operation and planning of numerous entities. A key function in power system operations and planning is the determination of total transfer capability (TTC), or the maximum amount of power that can be transferred from a set of source points to a set of sink points. This paper develops an algorithm for the decentralized computation of TTC through the application of the domain decomposition method (DDM). DDM decouples the correlation among interconnected control areas by taking advantage of the Schur complement matrix to form the power transfer distribution factor matrix. The decentralized TTC evaluation requires sparse information exchange among control areas. It is efficient and fully parallelizable. We demonstrate the decentralized TTC evaluation method on the IEEE 118-bus test case.**

***Index Terms*—Decentralized control, domain decomposition method, parallel computing, sensitivity analysis, total transfer capability.**

NOMENCLATURE:

n	system bus number
b	system branch number
$\boldsymbol{T}$	$n\times 1$ power transfer vector
$\boldsymbol{T}^{\text{source}}$	$n\times 1$ ATC power selling vector
$\boldsymbol{T}^{\text{sink}}$	$n\times 1$ ATC power purchasing vector
$h_{l,\boldsymbol{T}}$	the PTDF for a specific line l with respect to power transfer $\boldsymbol{T}$
p_l	the real power flow on line l in per unit
p	the scale of power transfer $\boldsymbol{T}$ in per unit
$TTC_{l,\boldsymbol{T}}$	the line-TTC value of line l with respect to power transfer $\boldsymbol{T}$
$\overline{p}_l$	the capacity of line l in per unit
$\boldsymbol{h_T}$	$b\times 1$ vector consisting of the PTDFs for all lines in the system
$\boldsymbol{H}$	$b \times n$ sensitivity matrix
$\boldsymbol{H}'$	$b \times (n-1)$ sensitivity matrix with the slack bus column removed from $\boldsymbol{H}$
$\boldsymbol{B}_{diag}$	$b \times b$ diagonal matrix consisting of line conductance
$\boldsymbol{M}$	$b \times (n-1)$ incidence matrix of the system with the slack bus removed
$\boldsymbol{B}_{bus}$	imaginary part of the $n \times n$ system admittance matrix
$\boldsymbol{B}'_{bus}$	$\boldsymbol{B}_{bus}$ with the slack bus row and column removed
$\boldsymbol{A}$	a general system solved by the DDM
k	the number of subsystems in $\boldsymbol{A}$
$\boldsymbol{R}$	the right-hand side of the problem $\boldsymbol{A}$
$\boldsymbol{B}, \boldsymbol{E}, \boldsymbol{F}, \boldsymbol{C}$	submatrices of system $\boldsymbol{A}$
$\boldsymbol{x}, \boldsymbol{y}$	submatrices of $\boldsymbol{X}$
$\boldsymbol{f}, \boldsymbol{g}$	submatrices of right-hand side $\boldsymbol{R}$
$\boldsymbol{B}_i, \boldsymbol{E}_i, \boldsymbol{F}_i$	submatrices of $\boldsymbol{B}$, $\boldsymbol{E}$ and $\boldsymbol{F}$
$\boldsymbol{f}_i, \boldsymbol{g}_i$	submatrices of $\boldsymbol{f}$ and $\boldsymbol{g}$
$\boldsymbol{S}$	the Schur complement matrix
$\boldsymbol{E}'_i, \boldsymbol{F}'_i$	submatrices of $\boldsymbol{E}'$ and $\boldsymbol{F}'$
$\boldsymbol{f}'_i, \boldsymbol{g}'_i$	submatrices of $\boldsymbol{f}'$ and $\boldsymbol{g}'$

Manuscript received July 11, 2014; revised February 06, 2015 and July 17, 2015; accepted October 05, 2015. Paper no. TPWRS-00947-2014.

The authors are with the School of Electrical and Computer Engineering, The Georgia Institute of Technology, Atlanta, GA 30332-0250 USA (e-mail: x.zhang@gatech.edu; xiaochenzhang8839@gmail.com; sgrijalva@ece.gatech.edu).

Color versions of one or more of the figures in this paper are available online at http://ieeexplore.ieee.org.

Digital Object Identifier 10.1109/TPWRS.2015.2493141

I. INTRODUCTION

THE electric grid is rapidly growing in complexity and control requirements. Since the beginnings of the digital computer and SCADA systems, the grid has been controlled using fundamentally centralized control approaches. However, as the demand for the deployment of distributed renewable energy grows, so does the need for the support of more sophisticated energy management and coordination across boundaries and subsystems. By leveraging advances in communication and smart-grid technologies, decentralized control strategies are seen as a scalable alternative to address control complexity and to further enhance system reliability and provide more flexibility for both energy providers and consumers through formal interaction mechanisms. ISOs, control area operators, distribution utilities, and facilities can acquire more capability for advanced decision-making after implementing decentralized control and computation strategies. Under a decentralized framework, entities that are coordinated properly can provide services that enhance system reliability, such as power reserves and better utilization of the grid capacity [1]. However, entities that are

not coordinated properly may make decisions that lead to reliability problems such as dynamic oscillations or cascading failures. Therefore, we must develop a secure and robust strategy for decentralized power system control and operation [2].

In electricity markets, both consumers and providers are entitled to trade electricity regardless of their locations, subject to the nodal price. To ensure the feasibility of electricity transactions, available transfer capability (ATC) is introduced. ATC is a measurement of the remaining physical electricity network capacity for further power transfers over already committed transactions [3]. Since the introduction of ATC, researchers have proposed many ATC evaluation methods, which can be categorized into DC power flow methods and AC power flow methods. One of the most frequently used DC power flow methods is power transfer distribution factors (PTDFs) method [4], which considers the line thermal limits for fast online ATC evaluation. AC power flow methods, such as continuation power flow method [5], optimal power flow method [6], and repeated power flow method [7], are slower but take the influence of reactive power flow and system voltage limits into consideration [8]. Mathematically, ATC can be derived by total transfer capability (TTC) minus various commitments and margins. This paper focuses on the TTC computation, which is the key element in ATC evaluation. During the TTC computation process, we consider line thermal limits and branch N-1 contingency constraints.

According to market regulations, entities do not need to disclose their network information. Therefore, a decentralized TTC evaluation method can ensure the feasibility of power transfers implemented across control areas. In addition, a decentralized TTC evaluation method will protect the confidentiality of each entity, which facilitates increased electricity trading while still maintains power system reliability. In sum, a decentralized TTC evaluation algorithm has the following potential advantages:

1) Protect information privacy of market participants;
2) Avoid additional investment in building central coordinators, supercomputers or data centers;
3) Promote parallel computing, which is much more computational efficient than centralized computing;
4) Enable coordination of control areas with different and distinct models;
5) Exhibit a lower system failure probability.

Researchers have proposed decentralized algorithms for various power system applications such as decentralized AC power flow [9], decentralized frequency control [2], and decentralized unit commitment [10]. However, the decentralized evaluation of TTC has not been the focus of recent studies. The major barrier for decentralized TTC evaluation is being able to decouple the correlations among control areas in the power system. That is, every power transfer has global influences, and must be analyzed and coordinated from a global point of view [11]. The physical correlation among control areas can also be mathematically interpreted as solving the inverse of system power flow Jacobian or its approximation by the reduced admittance matrix as a necessary step of TTC computation. The system admittance matrix consists of information blocks from all control areas. Under the decentralized control framework, the entire system admittance matrix will not be known. As a result, it is very difficult to solve the inverse of the admittance matrix in a decentralized manner.

To decentralize the TTC evaluation, researchers have proposed several approaches, which can be categorized into two categories. The first category introduces a two-level structure where a mega control system is built on top of the current control areas [12]. The mega system has the whole system information and is responsible to all computation that requires this information. Although the two-level structure protects the privacy of control areas by preventing direct information exchange among them, building such a mega system requires heavy investment on communication and computation infrastructure. The second category decentralizes the TTC computation by creating multiple area-level TTC problems where centralized TTC algorithm can be applied. The area-level TTC problem is formulated by decomposing the system into several area-level subsystems. To complete the topology of each subsystem, various system equivalents are added at the boundary buses. The adopted network equivalents include REI-equivalents [13], Kron reduction equivalents [14] and some fictitious nodes [15]. Although these methods do not require a mega system, the additional network equivalents and iterative processes slow down the algorithm and affect the accuracy of the result.

Compared with the above mentioned approaches, instead of finding a work-around of the centralized nature of TTC, this paper chooses to attack the problem directly by mathematically decentralizing the TTC evaluation algorithm itself using the domain decomposition method (DDM). The new algorithm can solve the inverse of the system admittance matrix in a decentralized manner without forming the complete admittance matrix. As a result, the new algorithm does not require building any mega system or making any system equivalents. The DDM-based algorithm can identify the least amount of information that needs to be shared among control areas which both allows an effective evaluation of TTC and protects the information privacy of each control area.

[16] is one of the first to explore the possibility of applying DDM to power system simulations, showing that DDM could be used as a preconditioner to improve computational efficiency in simulations of large synthetic circuit networks with millions of nodes. However, large realistic power systems usually only have about 10^4 nodes. Instead of studying the computational efficiency as in [16], this paper mainly focuses on the application of the DDM in decentralized power system control strategies. The TTC evaluation is fully parallelized through the DDM and further simplified by adopting a specific bus and branch reordering rule which considers the specific topological structure of a real power system. Compared with the centralized method, the proposed method can obtain the same results with higher computational efficiency in a decentralized manner.

The remainder of this paper is structured as follows: Section II discusses both the centralized and decentralized linear TTC evaluation methods, and Section III introduces the DDM as a decentralized control strategy for TTC evaluation. Section IV explains the DDM-based TTC evaluation method in detail through the IEEE 118-bus test case. Section V provides test results of the proposed algorithm and studies the effects

of system decomposition plans on computational efficiency. Section VI concludes the paper and discusses potential applications of the DDM in other decentralized power system control functions.

II. TTC Evaluation

A. Centralized TTC Evaluation

Let us first explore the centralized determination of TTC. A centralized linear TTC evaluation process implements power transfer distribution factors (PTDFs) to measure the sensitivity of the power flow on each transmission line with respect to a power transfer. For an n-bus, b-branch system, power transfer $\boldsymbol{T}$ as a vector is defined in (1).

$$\boldsymbol{T} = \boldsymbol{T}^{\text{source}} + \boldsymbol{T}^{\text{sink}}. \tag{1}$$

Then the PTDF for a specific line l with respect to a power transfer $\boldsymbol{T}$ is defined in (2).

$$h_{l,\boldsymbol{T}} = \frac{\partial p_l}{\partial p}. \tag{2}$$

As a result, the line TTC of line l can be calculated using (3),

$$TTC_{l,\boldsymbol{T}} = \begin{cases} \frac{\overline{p}_l - p_l}{h_{l,\boldsymbol{T}}} & h_{l,\boldsymbol{T}} > 0 \\ \frac{-\overline{p}_l - p_l}{h_{l,\boldsymbol{T}}} & h_{l,\boldsymbol{T}} < 0. \end{cases} \tag{3}$$

Finally, the global TTC value is determined by identifying the first line that hits its thermal limit.

The core for the TTC evaluation process described above is the computation of the PTDFs for all transmission lines or, in the matrix form, the PTDF vector ($\boldsymbol{h_T}$). For a power system with n buses and b branches, the PTDF vector can be derived using the sensitivity matrix $\boldsymbol{H}$ through (4) and (5) [17].

$$\boldsymbol{h_T} = \boldsymbol{HT}, \tag{4}$$

$$\boldsymbol{H'} = \boldsymbol{B}_{diag}\boldsymbol{M}\boldsymbol{B}'^{-1}_{bus}. \tag{5}$$

B. Decentralized TTC Evaluation

In a decentralized TTC evaluation algorithm, each control area has limited information about its neighbors. Each area performs area TTC analysis within its border and contributes to the global TTC result.

According to (4) and (5), if we assume the power transfer $\boldsymbol{T}$ is known, solving the PTDFs is equivalent to solving the sensitivity matrix $\boldsymbol{H}$. Once $\boldsymbol{H}$ is known, each control area can compute the line TTC using (3) independently and derive the area TTC, which is the minimum value of line TTC. The global TTC value is determined by the minimum area TTC. We can formulate the decentralized TTC evaluation problem as a problem of solving the sensitivity matrix $\boldsymbol{H}$ in a decentralized manner.

To simplify (5), let us designate

$$\overline{\boldsymbol{B}} = \left(\boldsymbol{B}_{diag}\boldsymbol{M}\right)^T, \tag{6}$$

$$\overline{\boldsymbol{A}} = \boldsymbol{B}'^T_{bus}, \tag{7}$$

$$\text{and} \quad \boldsymbol{X} = \boldsymbol{H}'^T. \tag{8}$$

Then, the computation of $\boldsymbol{H'}$ is equivalent to solving the following system (9) for $\boldsymbol{X}$.

$$\overline{\boldsymbol{A}}\boldsymbol{X} = \overline{\boldsymbol{B}}. \tag{9}$$

According to (7), solving (9) in a decentralized manner is not easy, because it requires us to compute the inverse of the system admittance matrix $\boldsymbol{B}'_{bus}$, which consists of information blocks from all control areas. In the next section, we show the DDM-based algorithm can solve the system (9) without forming the complete $\boldsymbol{B}'_{bus}$ matrix.

III. Domain Decomposition Method

DDM is an algorithm originally developed for structural engineering based on the philosophy of divide-and-conquer [18]. Recently, due to the continuous development of modern multiprocessor computing technology, researchers have proven that the DDM is very effective at solving various problems in large systems written in form of (10).

$$\boldsymbol{AX} = \boldsymbol{R}. \tag{10}$$

To apply the DDM, we must decompose the studied system $\boldsymbol{A}$ into several subsystems. For a given interconnected system, let's assume that the network could be decomposed into k subsystems. After reordering, we can rewrite the system (10) into (11) and solve for $\boldsymbol{x}$ and $\boldsymbol{y}$ [18]:

$$\boldsymbol{AX} = \begin{pmatrix} \boldsymbol{B} & \boldsymbol{E} \\ \boldsymbol{F} & \boldsymbol{C} \end{pmatrix} \begin{pmatrix} \boldsymbol{x} \\ \boldsymbol{y} \end{pmatrix} = \boldsymbol{R} = \begin{pmatrix} \boldsymbol{f} \\ \boldsymbol{g} \end{pmatrix}, \tag{11}$$

where

$$\boldsymbol{AX} = \begin{pmatrix} \boldsymbol{B}_1 & & & & \boldsymbol{E}_1 \\ & \boldsymbol{B}_2 & & & \boldsymbol{E}_2 \\ & & \ddots & & \vdots \\ & & & \boldsymbol{B}_k & \boldsymbol{E}_1 \\ \boldsymbol{F}_1 & \boldsymbol{F}_2 & \dots & \boldsymbol{F}_k & \boldsymbol{C} \end{pmatrix} \begin{pmatrix} \boldsymbol{x}_1 \\ \boldsymbol{x}_2 \\ \vdots \\ \boldsymbol{x}_k \\ \boldsymbol{y} \end{pmatrix}, \text{ and } \boldsymbol{R} = \begin{pmatrix} \boldsymbol{f}_1 \\ \boldsymbol{f}_2 \\ \vdots \\ \boldsymbol{f}_k \\ \boldsymbol{g} \end{pmatrix}.$$

The DDM solves the system (11) in a decentralized manner through five standard steps:

ALGORITHM: Domain Decomposition Method

1. Solve $\boldsymbol{BE'} = \boldsymbol{E}$, and $\boldsymbol{Bf'} = \boldsymbol{f}$ for $\boldsymbol{E'}$ and $\boldsymbol{f'}$, respectively
2. Compute $\boldsymbol{g'} = \boldsymbol{g} - \boldsymbol{Ff'}$
3. Compute $\boldsymbol{S} = \boldsymbol{C} - \boldsymbol{FE'}$
4. Solve $\boldsymbol{Sy} = \boldsymbol{g'}$ for $\boldsymbol{y}$
5. Compute $\boldsymbol{x} = \boldsymbol{f'} - \boldsymbol{E'y}$ for $\boldsymbol{x}$

Equation (10)–(11) shows that the DDM rewrites the system $\boldsymbol{A}$ as a new matrix in block form. $\boldsymbol{S}$ is called Schur complement matrix. Compared with solving the inverse of $\boldsymbol{A}$ directly, the DDM solves the inverse of $\boldsymbol{B}$ (a block diagonal matrix) and $\boldsymbol{S}$ (with a much lower dimension), which is substantially easier. Although the DDM has great potential for enhancing computing efficiency [16], this paper emphasizes its decentralized computing property.

IV. Application of the DDM to Distributed TTC Evaluation

To illustrate how DDM is applied to the TTC evaluation, we adopt the IEEE 118-bus test case. The test case consists of 118 buses and 186 branches.

A. System Decomposition and Reordering

Before the application of the DDM, all studied systems must first go through the process of decomposition and reordering.

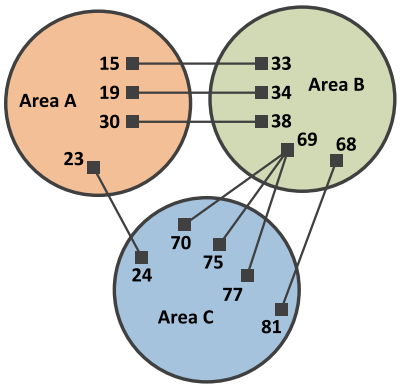

Fig. 1. IEEE 118 Case System Decomposition Results [14].

TABLE I
IEEE 118-BUS SYSTEM DECOMPOSITION.

Control Area	Bus ID
Area A	1~23, 25~32, 113~115, 117
Area B	33~69, 116
Area C	24, 70~112, 118

Researchers have developed three basic types of system decomposition methods: vertex-based, edge-based, and element-based decomposition [18]. In power system analysis, because all buses are assigned to their corresponding control areas and all control areas are connected through a few tie lines, vertex-based partition is ideal. Thus, we decompose the IEEE 118-bus system into three control areas using vertex-based partition method according to Table I. Several tie lines connect each control area to its neighbors, shown in Fig. 1.

After system decomposition, we need to reorder the bus and branch IDs in order to write the system in the block matrix form as shown in (11). To begin with, we rank the control areas in an arbitrary order, such as A, B, C, and so on. During the reordering process, all buses and branches are ranked according to their corresponding control area. Buses and branches belong to the same control area are always ranked consecutively. Then, we further classify all buses into two categories: internal buses and boundary buses, and all branches into internal branches and tie lines. Fig. 1 shows that the decomposition of the IEEE 118-bus test case results in 14 boundary buses and 8 tie lines in total. We rank internal buses before boundary buses and internal branches before tie lines.

In the 118-bus case example, after reordering the 118 buses and 186 branches, we will have the matrix of $\overline{\boldsymbol{A}}$ and $\overline{\boldsymbol{B}}$ in (9) following a specific form as shown in Figs. 2 and 3. Matrix $\overline{\boldsymbol{A}}$ follows the exact block matrix pattern as $\boldsymbol{A}$ in (11). However, unlike the general system $\boldsymbol{A}$, in power system $\overline{\boldsymbol{A}}$, we can further show that the gray sub-blocks in $\boldsymbol{E}$ and $\boldsymbol{F}$ are empty because internal buses can only be connected to the boundary buses in the same control area, shown in Fig. 2. This special pattern of the $\boldsymbol{E}$ and $\boldsymbol{F}$ block matrices in power system $\overline{\boldsymbol{A}}$ plays a vital role in the parallel application of the DDM. Block $\boldsymbol{C}$ in $\overline{\boldsymbol{A}}$ represents that the boundary buses are connected with each other through a series of tie lines.

Fig. 3 illustrates the structure of the right-hand side matrix $\overline{\boldsymbol{B}}$ in (9). Compared with (11), which only has a single right-hand side in $\boldsymbol{R}$, (9) has multiple right-hand sides. Every row in the right-hand side matrix $\overline{\boldsymbol{B}}$ stands for a bus in the system, and every column in $\overline{\boldsymbol{B}}$ corresponds to a branch which connects two buses. According to the characteristics of the real power system topology, $\boldsymbol{g}$ is a block diagonal matrix. $\boldsymbol{f}_4$ is empty because tie lines only connect boundary buses. If we do not reorder the bus and branch IDs according to the rules mentioned above, we cannot rewrite the system equation suitable for the DDM. That is, we will not have $\boldsymbol{E}$, $\boldsymbol{F}$ and $\boldsymbol{g}$ matrices in (11) written in the diagonal-block form.

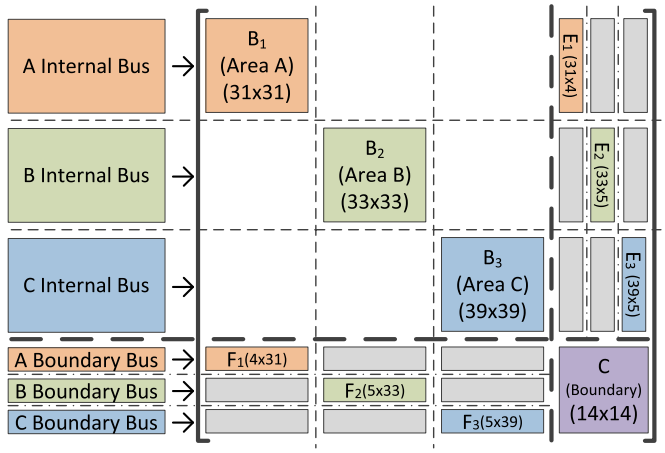

Fig. 2. Matrix $\overline{\boldsymbol{A}}$ Structure and Bud ID Reordering Results.

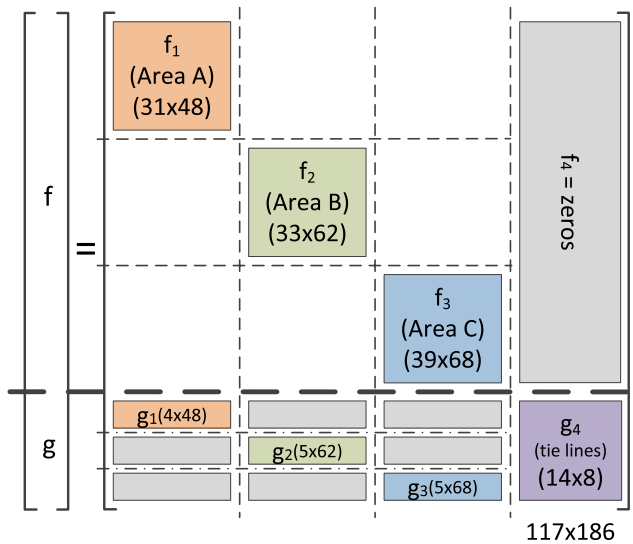

Fig. 3. Right-hand sides $\overline{\boldsymbol{B}}$ Structure and Branch ID Reordering Results.

In a decentralized TTC computation algorithm, each control area only possesses its own network information. In this paper, we emphasis the possession of the network information with different colors: red blocks stand for information possessed by control area A; green blocks for control area B, blue blocks for control area C, and purple blocks for tie line information assumed to be available by all control areas.

B. Sensitivity Matrix Computation Using the DDM

After system decomposition and element ID reordering, the DDM can be applied to compute the sensitivity matrix $\boldsymbol{H}$ by solving (9) in a decentralized manner. Similar to the standard

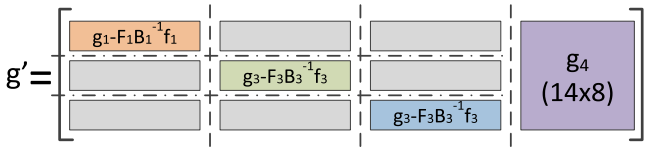

Fig. 4. Structure of Matrix $\boldsymbol{g}'$.

DDM algorithm shown in Section III, the sensitivity matrix $\boldsymbol{H}$ computation consists of five steps.

Step 1: Solve $\boldsymbol{BE}' = \boldsymbol{E}$ and $\boldsymbol{Bf}' = \boldsymbol{f}$ for $\boldsymbol{E}'$ and $\boldsymbol{f}'$:

According to Fig. 2, where

$$\boldsymbol{B} = diag\left(\boldsymbol{B}_1, \boldsymbol{B}_2, \boldsymbol{B}_3\right) \quad \text{and} \tag{12}$$

$$\boldsymbol{E} = diag\left(\boldsymbol{E}_1, \boldsymbol{E}_2, \boldsymbol{E}_3\right), \tag{13}$$

we immediately get

$$\boldsymbol{E}' = diag\left(\boldsymbol{E}\prime_1, \boldsymbol{E}'_2, \boldsymbol{E}'_3\right), \tag{14}$$

where $\boldsymbol{E}'_i = {\boldsymbol{B}_i}^{-1}\boldsymbol{E}_i$, $i = 1, 2, 3$. Similarly, if we ignore the empty matrix $\boldsymbol{f}_4$ in Fig. 3, we can get

$$\boldsymbol{f}' = \left[diag\left(\boldsymbol{f}'_1, \boldsymbol{f}'_2, \boldsymbol{f}'_3\right), \boldsymbol{f}_4\right], \tag{15}$$

where $\boldsymbol{f}'_i = \boldsymbol{B}_i^{-1}\boldsymbol{f}_i$, $i = 1, 2, 3$.

Since we can reuse the LU decomposition of $\boldsymbol{B}$ when solving $\boldsymbol{E}'$ and $\boldsymbol{f}'$, in practice, we usually solve the two systems simultaneously [16]. Step 1 is fully parallelizable for each control area, because no neighboring control area information is involved in the process.

Step 2: Compute $\boldsymbol{g}' = \boldsymbol{g} - \boldsymbol{Ff}'$:

According to Figs. 2 and 3 where

$$\boldsymbol{g} = [diag\left(\boldsymbol{g}_1, \boldsymbol{g}_2, \boldsymbol{g}_3\right), \boldsymbol{g}_4], \quad \text{and} \tag{16}$$

$$\boldsymbol{F} = diag(\boldsymbol{F}_1, \boldsymbol{F}_2, \boldsymbol{F}_3), \tag{17}$$

we can immediately obtain $\boldsymbol{g}' = [diag\left(\boldsymbol{g}'_1, \boldsymbol{g}'_2, \boldsymbol{g}'_3\right), \boldsymbol{g}_4]$, where $\boldsymbol{g}'_i = \boldsymbol{g}_i - \boldsymbol{F}_i\boldsymbol{f}'_i$, $i = 1, 2, 3$. The structure of $\boldsymbol{g}'$ is shown in Fig. 4. Similar to step 1, step 2 is also fully parallelizable.

Step 3: Compute $\boldsymbol{S} = \boldsymbol{C} - \boldsymbol{FE}'$:

According to [18], $\boldsymbol{S}$ is the Schur complement matrix associated with $\boldsymbol{y}$. In a power system, the size of the Schur complement matrix is determined by the total number of boundary buses in all control areas. To solve $\boldsymbol{Sy} = \boldsymbol{g}'$ in parallel in the step 4, control areas must share some information to form the Schur complement matrix. In the 118-bus test case, the Schur complement matrix is shown in Fig. 5. Since block matrix $\boldsymbol{C}$ (tie line information in Fig. 2) is known to all control areas, the information that requires sharing is $\boldsymbol{F}_1\boldsymbol{E}'_1$, $\boldsymbol{F}_2\boldsymbol{E}'_2$ and $\boldsymbol{F}_3\boldsymbol{E}'_3$, all of which are very small square matrices (4×4, 5×5 & 5×5) that can be computed within each control area independently.

Step 4: Solve $\boldsymbol{Sy} = \boldsymbol{g}'$:

When the Schur complement matrix is ready, according to the structure of $\boldsymbol{g}'$, $\boldsymbol{y}$ can be solved in parallel, shown in Fig. 6.

Step 5: Compute $\boldsymbol{x} = \boldsymbol{f}' - \boldsymbol{E}'\boldsymbol{y}$:

To compute $\boldsymbol{x}$ in parallel, control areas must share $\boldsymbol{E}'_i$ before solving $\boldsymbol{E}'\boldsymbol{y}$. Let $\boldsymbol{x}' = \boldsymbol{E}'\boldsymbol{y}$. According to the structures of $\boldsymbol{E}'$ and $\boldsymbol{y}$, we further simplify the matrix product of $\boldsymbol{E}'\boldsymbol{y}$ by rewriting the matrix $\boldsymbol{y_i}$ in Fig. 6 as $\boldsymbol{y}_i = [\boldsymbol{y}_{i1}; \boldsymbol{y}_{i2}; \boldsymbol{y}_{i3}; \boldsymbol{y}_{i4}]$. Fig. 7 shows how the matrix product $\boldsymbol{x}' = \boldsymbol{E}'\boldsymbol{y}$ is computed in parallel. Once $\boldsymbol{x}'$ is known, $\boldsymbol{x}$ can be computed through $\boldsymbol{x} = \boldsymbol{f}' - \boldsymbol{x}'$, which is also fully parallelizable.

Finally, the sensitivity matrix $\boldsymbol{H}' = \boldsymbol{X}^T = [\boldsymbol{x}^T; \boldsymbol{y}^T]$. By adding the slack bus (add one zero column) to $\boldsymbol{H}'$, we obtain the $b \times n$ sensitivity matrix $\boldsymbol{H}$, shown in Fig. 8.

Each row of $\boldsymbol{H}$ represents the sensitivity information of a specific branch. Since we solve $\boldsymbol{H}$ in a decentralized manner, each control area only knows a part of the $\boldsymbol{H}$ matrix, except tie line sensitivities which are known by all control areas. This is indicated by different color blocks in Fig. 8. Control areas will use the sensitivity matrix $\boldsymbol{H}$ to form branch PTDFs and then calculate line TTC and area TTC.

One of the major contributions of this paper is decentralization of the sensitivity matrix calculation using DDM. Fig. 9 shows how DDM is implemented to compute the $\boldsymbol{H}$ matrix for an interconnected system consisting of k control areas. To simplify the algorithm, we marked the entire $\boldsymbol{H}$ computation

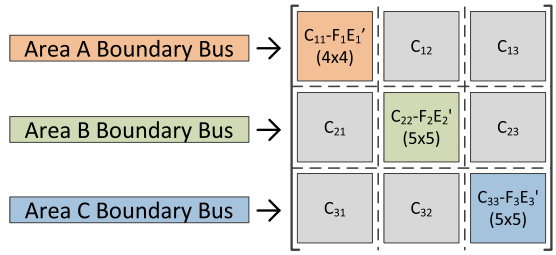

Fig. 5. Schur Complement Matrix $\boldsymbol{S}$.

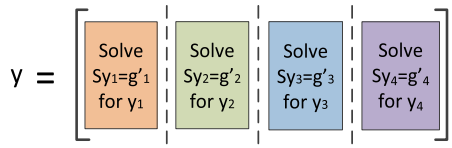

Fig. 6. $\boldsymbol{y}$ Matrix Structure.

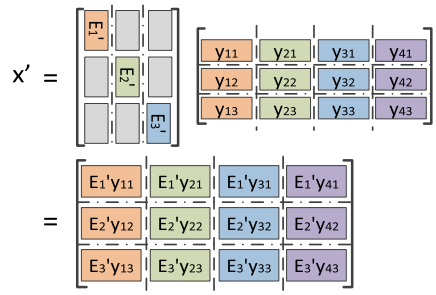

Fig. 7. Sensitivity Matrix $\boldsymbol{S}'$ Computing Flow Chart.

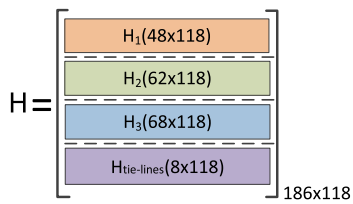

Fig. 8. Sensitivity Matrix $\boldsymbol{H}$.

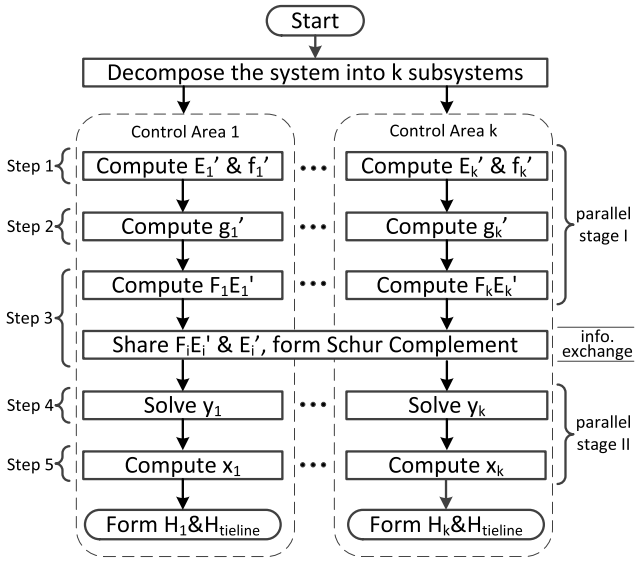

Fig. 9. The Computation of Sensitivity Matrix $\boldsymbol{H}$.

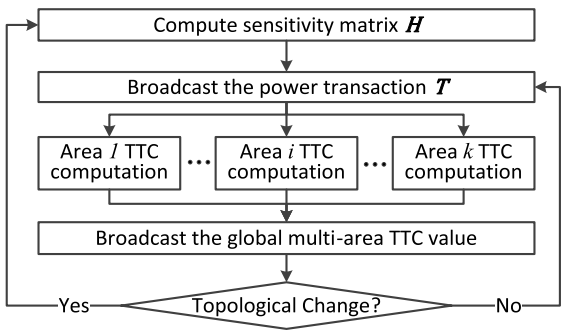

Fig. 10. Multi-area Coordination for Decentralized TTC Computation.

process with 5 steps correspond to the 5-step algorithm of the standard DDM shown in Section III.

To illustrate the information flow among control areas, we divided the algorithm into two parallel stages with an information exchange stage. During the parallel stages, there is no information exchange among control areas. However, during information exchange stage, two pieces of information ($\boldsymbol{F}_i\boldsymbol{E'}_i$ *and* $\boldsymbol{E'}_i$) must be shared in order to form the Schur complement matrix $\boldsymbol{S}$ and compute $\boldsymbol{y}$. As mentioned in step 3 and step 5, both $\boldsymbol{F}_i\boldsymbol{E'}_i$ *and* $\boldsymbol{E'}_i$ are of very small sizes compared with the whole system matrix $\overline{\boldsymbol{A}}$.

C. Global TTC Evaluation Coordination and Computational Compatibility

Since the TTC evaluation requires some information exchange among control areas, certain coordination is necessary. Such coordination is shown in Fig. 10, where the flow chart of TTC evaluation is demonstrated.

Because the DDM seeks to mathematically decentralize the TTC computation, the problem formulation of the DDM-based TTC evaluation is no different than traditional TTC problem formulation except the TTC value is computed in a decentralized manner. Fig. 10 shows how multiple control areas coordinate to compute the global TTC value, where solving the sensitivity matrix $\boldsymbol{H}$ is the first step. Once the sensitivity matrix is known, each control area could calculate the area TTC value through (3). The global TTC is the minimum value of area TTC. Moreover, by definition, the sensitivity matrix $\boldsymbol{H}$ is subject to system topology changes. As a result, the sensitivity matrix $\boldsymbol{H}$ needs update whenever the system topology changes.

According to Figs. 9 and 10, we can summarize all the exchanged information among control areas:

(i) Power transaction information $\boldsymbol{T}$
(ii) Matrix product $\boldsymbol{F}_i\boldsymbol{E'}_i$ and $\boldsymbol{E'}_i$
(iii) Area TTC value

Compared with other decentralized TTC evaluation algorithms, the DDM-based algorithm does not require sensitive information exchange among control areas. Even the shared matrix product $\boldsymbol{F}_i\boldsymbol{E'}_i$ and matrix $\boldsymbol{E'}_i$ cannot be extrapolated by others to derive internal sensitive information of the control area. As a result, the proposed algorithm perfectly protects the information privacy of all involved entities.

Another advantage of the proposed DDM-based algorithm is its compatibility with other computational methods that exploit the power system sparsity, including direct methods such as Gaussian elimination, LU decomposition, and Cholesky factorization as well as iterative methods such as generalized minimal residual method (GMRES), minimum residual method (MINRES) and conjugate gradient method (CG). This is because in the DDM the block matrices generated by system decomposition such as $\boldsymbol{B}_i$, $\boldsymbol{E}_i$, $\boldsymbol{F}_i$, $\boldsymbol{f}_i$, and $\boldsymbol{g}_i$ remain sparse, and square matrices such as $\boldsymbol{B}_i$ bear the same symmetric or positive definite properties as the original matrix $\overline{\boldsymbol{A}}$. As a result, the proposed algorithm is compatible with other sparse computational methods.

TABLE II
IEEE 118-BUS SYSTEM LINE CAPACITY.

Transmission Lines	Capacity
1,2,4,6,10,12,14~20,22,24~30,34,35,39,40,42~49,52,53,55~59 ,91, 92,100, 101,103~106,109,111~115,117,118,120~122,125,126, 128~133,135,136,140, 143~162,164~182,184~186	150MW
3,5,11,13,21,23,31,33,37,38,41,50,90,94,96~99,108,110,116,1 19,123,124, 137~139,141,142,163,183	800MW
7~9,32,36,51,54,93,95,102,107,127,134	1000MW

Note: all transmission lines are considered as double-circuit lines.

V. TEST RESULTS

A. IEEE 118 Case

Since the original IEEE 118-bus test case does not include transmission line capacities, we modified the system by adding them (see Table II). After modification, the test case is verified to be N-1 secure, which indicates that the system admittance matrix is always invertible.

B. DDM-Based TTC Evaluation Method

We implemented both the traditional centralized and DDM-based decentralized algorithms to calculate TTC for the IEEE 118-bus test case. N-1 contingency constraint is enforced. Table III shows the two algorithms yield the same TTC evaluation result. This verifies the accuracy of the DDM-based algorithm.

We also compare the computational efficiency of the two TTC evaluation algorithms by recording their computation time. In

TABLE III
TTC CALCULATION RESULTS CONSIDERING N-1 CONTINGENCIES (MW).

Trans ID	From Bus	To Bus	TTC[1]	TTC[2]	ERR‰
1	69	2	208.7876	208.7876	9.5289e-15
2	69	101	169.8244	169.8244	1.6569e-14
3	100	7	150.2845	150.2845	1.4184e-14
4	113	50	77.8638	77.8638	3.6502e-16
5	6	110	68.3661	68.3661	9.9775e-15

a. TTC[1]: centralized TTC evaluation results.
b. TTC[2]: DDM-based decentralized TTC evaluation results.

TABLE IV
SENSITIVITY MATRIX CALCULATION EFFICIENCY COMPARISON.

Time(*ms*)	Parallel Stage I			Parallel Stage II		DDM	Cent.
	Step1	Step2	Step3	Step4	Step5		
Area A	0.0771	0.0198	0.0145	0.1588	0.1854	0.5348	0.6733
Area B	0.0911	0.0237	0.0124	0.1822	0.2186		
Area C	0.0982	0.0194	0.0119	0.1734	0.2319		
Tie lines	--	--	--	0.0662	0.0527		

a. The 'tie lines' computation time in steps 4 and 5 refer to the computation time of solving y_4 and $H_{tielines}$ in Fig. 6 and Fig. 8 respectively.

Table IV, columns "DDM" and "Cent" stand for the total computation time of $\boldsymbol{H}'$ using the DDM-based algorithm and the centralized algorithm, respectively. System component failures are not considered in the efficiency evaluation. In Table IV, the computation time for each of the five steps in the DDM-based algorithm is shown for all three control areas. We assume that tie-line information is known by all control areas, so they could share the tie line computing burden in step 4 and step 5. Due to parallel computing, the total computation time of the DDM-based method is the sum of the parallel stages I and II, shown in Fig. 9. The computation time for both parallel stage I and II is determined by the longest computation time among all control areas. Under the system decomposition plan shown in Table I, control area C is the slowest among all control areas, so it becomes a bottleneck that determines the overall computational efficiency of the algorithm.

Researchers and engineers typically use the DDM to solve large systems with millions of variables in which direct methods such as LU factorization or iterative methods such as generalized minimal residual method (GMRES) are ineffective. That is, they use the DDM only to improve computational efficiency. However, in power system analysis, the size of a system is relatively small (around $10^4 \times 10^4$). As a result, apart from improving computational efficiency, more importantly, the DDM allows decentralized control and parallelized computation in power industry. In Table IV, if all computations from all control areas are performed by one processor, the DDM-based algorithm could be slower than the centralized algorithm. However, if we allocate the computational burden of the DDM to multiple processors among control areas through parallel computing, the computation time of the DDM-based algorithm becomes shorter than that of the centralized method, even in small power systems. Given that each control area already has its own computing capability, we conclude that the decentralized method outperforms the centralized method in both parallel computing capability and computational efficiency.

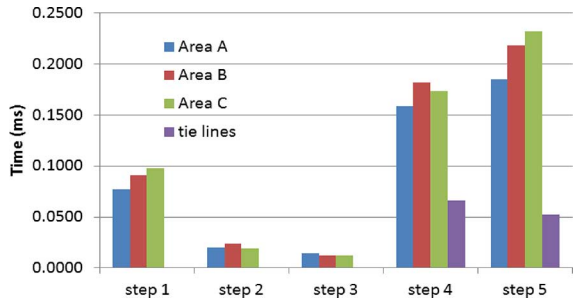

Fig. 11. Computation Time for Each Step Among All Control Areas.

TABLE V
IEEE 118-BUS SYSTEM DECOMPOSITION PLAN II.

Control Area	Bus ID
Area *A*	1~19, 27~32, 113~115, 117
Area *B*	20~26, 65, 68~81, 97~99, 116, 118
Area *C*	33~64, 66, 67
Area *D*	82~96, 100~112

TABLE VI
IEEE 118-BUS SYSTEM DECOMPOSITION PLAN III.

Control Area	Bus ID
Area *A*	1~19, 28~36, 113, 117
Area *B*	20~27, 49, 62, 65~76, 87~81, 99, 114~116, 118
Area *C*	37~48, 50~61, 63, 64
Area *D*	77, 82~98, 100~112

Fig. 11 shows that the computational burden among control areas is not allocated evenly under the current system decomposition plan, in which area C is a bottleneck in efficiency. Thus, a better system decomposition plan that allocates the computational burden more evenly among control areas will enable the DDM to achieve higher overall efficiency. The next section further examines the influences of system decomposition plan on the efficiency of the DDM-based algorithm.

C. Further Examination of System Decomposition

Power system decomposition is a conventional problem that has been studied by many power system engineers and mathematicians. The most commonly used power system decomposition methods include Lagrangian-based method [19], optimality condition decomposition method [20], [21] and electrical distance based method [22]. However, none of these existing decomposition methods are optimized for the DDM-based TTC evaluation. As a result, the TTC performance of these decomposition methods [10], [21], [23] varies from case to case, and it is very difficult to conclude whether one method is consistently better than the other.

Although there is no existing optimized decomposition method for the DDM-based TTC evaluation, there are two key characteristics which determine the goodness of a system decomposition. We illustrate the two key characteristics through three distinct system decomposition examples. Plan I decomposes the system into three control areas according to Table I, and plans II and III decompose the system into four control

TABLE VII
SYSTEM DECOMPOSITION PLANS COMPARISON.

Bus ID	Total Bus / Boundary Bus				Tie Lines	Schur Complement Size
	A	*B*	*C*	*D*		
Plan I	35/4	38/5	45/5	--/--	8	14 x 14
Plan II	29/5	27/11	34/7	28/3	17	26 x 26
Plan III	30/7	31/14	26/13	31/5	35	39 x 39

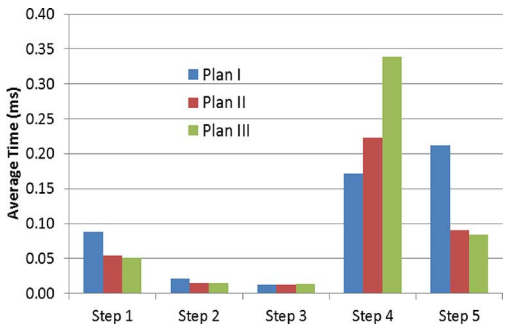

Fig. 12. Computation time for Each Step Among All Control Areas.

areas according to Tables V and VI. Table VII shows the bus and tie line information of all control areas under the three system decomposition plans.

Comparing plans I, II, and III, we can see that an increased number of control areas will usually lead to more boundary buses and more tie lines. We can also see that when the numbers of control areas are the same in both plans II and III, a good decomposition plan will result in smaller numbers of boundary buses and tie lines. Since the number of boundary buses determines the size of the Schur complement matrix, the fewer boundary buses there are, the more efficient the algorithm will be.

Table VIII shows the computation time of the three system decomposition plans. Fig. 12 provides a comparison of the average area computation time of each step for the three system decomposition plans.

According to Table VIII, plan II outperforms the other two plans in computational efficiency. As the number of the control area increases, the computational burden for each sub-system decreases. Thus, steps 1 and 5 will take considerably less time, which explains why plan II outperforms plan I. On the other hand, an increased number of control areas will lead to an increased number of boundary buses which further increases the size of the Schur complement matrix. Fig. 13 shows the Schur complement matrices and their non-zero elements for all three decomposition plans respectively. Compared to other system block matrices $\boldsymbol{B}_i$, the Schur complement matrix $\boldsymbol{S}$ is usually much denser and more expensive to solve. As a result, when Schur complement matrix becomes too large, solving $\boldsymbol{Sy} = \boldsymbol{g}'$ in step 4 becomes very time consuming and inefficient, which explains why plan III experiences an extensive computation time on step 4.

The overall efficiency of the DDM-based TTC evaluation algorithm relies on how the system is decomposed. Although

TABLE VIII
COMPARISONS OF COMPUTING EFFICIENCIES (MS).

Plan I	**Parallel I**	**Parallel II**	**Total time**
Area A	0.1063	0.3493	0.5348
Area B	0.1221	0.4058	
Area C	0.1245	0.4104	
Plan II	**Parallel I**	**Parallel II**	**Total time**
Area A	0.0865	0.3201	0.4558
Area B	0.0623	0.2835	
Area C	0.0894	0.3664	
Area D	0.0697	0.3057	
Plan III	**Parallel I**	**Parallel II**	**Total time**
Area A	0.0926	0.4657	0.5582
Area B	0.0638	0.4101	
Area C	0.0603	0.3936	
Area D	0.0757	0.4510	

a. The bold case numbers are used to calculate total time in DDM.

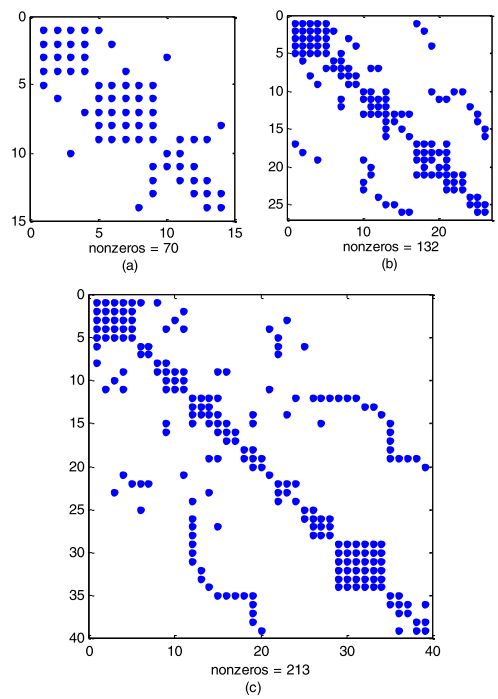

Fig. 13. Schur Complement Matrices for Plans I, II, and III, Respectively. (a) Schur Complement Matrix for Plan I. (b) Schur Complement Matrix for Plan II. (c) Schur Complement Matrix for Plan III.

there is no existing decomposition method for our specific purpose, an efficient decomposition plan should follow two key rules:

(i) The system decomposition plan must balance the number of control areas and the number of boundary buses. If the number of control areas is fixed, an efficient plan has fewer boundary buses.

(ii) The system decomposition plan must balance the sizes of the control areas. In other words, the bus and branch

numbers of a control area should be proportional to its computational capability.

VI. Conclusion

In this paper, we proposed a novel algorithm to decentralize the power system TTC evaluation process using the DDM. Unlike other decentralized algorithms examined, the proposed algorithm attacks the problem mathematically by decentralizing the TTC matrix computation itself. The DDM-based algorithm can obtain the same numerical results as the centralized method with less computation time.

Since the DDM mathematically decouples the correlations among control areas when inversing the system matrix, we can easily implement the DDM to decentralize many other power system applications [24] such as contingency analysis, real-time security-constrained dispatch, day-ahead security-constrained unit commitment, state estimation, and AC power flow analysis. In the future, an optimized system decomposition method will further enhance the computational efficiency of the decentralized TTC evaluation algorithm.

References

[1] A. Adamson, A. Dessel, and L. Garver, "Generation reserve value of interconnections," *IEEE Trans. Power App. Syst.*, vol. PAS-96, no. 2, pp. 337–346, 1977.

[2] M. H. Nazari, Z. Costello, M. J. Feizollahi, S. Grijalva, and M. Egerstedt, "Distributed frequency control of prosumer-based electric energy systems," *IEEE Trans. Power Syst.*, vol. 29, no. 6, pp. 2934–2942, Nov. 2014.

[3] Available Transfer Capability Definition and Determination. Princeton, NJ, USA, North American Electric Reliability Council (NERC), 1996.

[4] S. Grijalva, P. W. Sauer, and J. D. Weber, "Enhancement of linear ATC calculations by the incorporation of reactive power flows," *IEEE Trans. Power Syst.*, vol. 18, no. 2, pp. 619–624, May 2003.

[5] M. Shaaban, W. Li, Z. Yan, Y. Ni, and F. Wu, "Calculation of total transfer capability incorporating the effect of reactive power," *Electr. Power Syst. Res.*, vol. 64, no. 3, pp. 181–188, 2003.

[6] E. D. Tuglie, M. Dicorato, M. L. Scala, and P. Scarpellini, "A static optimization approach to access dynamic available transfer capability," *IEEE Trans. Power Syst.*, vol. 15, no. 3, pp. 1069–1076, Aug. 2000.

[7] B. Gao, G. Morison, and P. Kundur, "Towards the development of a systematic approach for voltage stability assessment of large-scale power systems," *IEEE Trans. Power Syst.*, vol. 11, no. 3, pp. 1314–1324, Aug. 1996.

[8] C. A. Canizares, A. Berizzi, and P. Marannino, "Using FACTS controllers to maximize available transfer capability," in *Proc. 1998 Bulk Power Systems Dynamics and Control IV-Restructuring*, pp. 633–641.

[9] E. Granada, M. J. Rider, J. R. S. Mantovani, and M. Shahidehpour, "Decentralized AC power flow for real-time multi-TSO power system operation," in *Proc. 2010 IEEE Power and Energy Soc. General Meeting*, pp. 1–7.

[10] L. Mingyang and P. B. Luh, "A decentralized framework of unit commitment for future power markets," in *Proc. 2013 IEEE Power and Energy Soc. General Meeting*, pp. 1–5.

[11] L. Yuan and V. Venkatasubramanian, "Coordination of transmission path transfers," *IEEE Trans. Power Syst.*, vol. 19, no. 3, pp. 1607–1615, Aug. 2004.

[12] L. Zhao and A. Abur, "Two-layer multi-area total transfer capability computation," in *Proc. 2004 IREP Symp.*, Cortina D'Ampezzo, Italy, 2004.

[13] M. Liang and A. Abur, "REI-equivalent based decomposition method for multi-area TTC computation," in *Proc. 2006 IEEE PES Transmission and Distribution Conf. Exhib.*, pp. 506–510.

[14] X. Zhang and S. Grijalva, "Multi-area TTC evaluation based on Kron reduction," in *Proc. 2013 IEEE Smart Energy Grid Engineering*, vol. 1, no. 6, pp. 28–30.

[15] A. A. Khatir, V. Etard, and R. Cherkaoui, "Assessment of total transfer capability for simultaneous transactions in decentralized multi-areas power systems," in *Proc. 2012 IEEE Power and Energy Soc. General Meeting*, pp. 1–6.

[16] Q. Zhou, K. Sun, K. Mohanram, and D. C. Sorensen, "Large power grid analysis using domain decomposition," in *Proc. 2006 Design, Automation and Test in Europe*, vol. 1, no. 6, pp. 6–10.

[17] X. Wang, Y. Song, and M. Irving, *Modern Power System Analysis*. Beijing, China: Science Press, 2012, pp. 246–248.

[18] Y. Saad, *Iterative Methods for Sparse Linear Systems*. Philadelphia, PA, USA: SIAM, 2003, pp. 469–475.

[19] B. H. Kim and R. Baldick, "A comparison of distributed optimal power flow algorithms," *IEEE Trans. Power Syst.*, vol. 15, no. 2, pp. 599–604, May 2000.

[20] F. J. Nogales, F. J. Prieto, and A. J. Conejo, "A decomposition methodology applied to the multi-area optimal power flow problem," *Ann. Oper. Res.*, vol. 120, no. 1–4, pp. 99–116, 2003.

[21] J. Guo, G. Hug, and O. Tonguz, "Impact of partitioning on performance of decomposition methods for AC optimal power flow," in *Proc. Conf. 2015 IEEE Innovative Smart Grid Technologies*.

[22] E. Cotilla-Sanchez, P. D. H. Hines, C. Barrows, S. Blumsack, and M. Patel, "Multi-attribute partitioning of power networks based on electrical distance," *IEEE Trans. Power Syst.*, vol. 28, no. 4, pp. 4979–4987, Nov. 2013.

[23] G. Karypis and V. Kumar, "A fast and high quality multilevel scheme for partitioning irregular graphs," *SIAM J. Sci. Comput.*, vol. 20, no. 1, pp. 359–392, 1998.

[24] B. Stott, J. Jardim, and O. Alsaç, "DC power flow revisited. Power systems," *IEEE Trans. Power Syst.*, vol. 24, no. 3, pp. 1290–1300, Aug. 2009.

Xiaochen Zhang received a B.S. degree at Xi'an Jiaotong University (2010) and dual M.S. degrees at both Shanghai Jiao Tong University and Georgia Tech (2013). He is currently a Ph.D. Student and research assistant at the Advanced Computational Electricity Systems (ACES) Laboratory in the School of Electrical and Computer Engineering at Georgia Tech.

He has been involved in various research projects on power system data analytics supported by PSERC, Georgia Tech, and the Southern Company. He has also undertaken a power system planning project funded by China State Grid, Inc., that integrates the Gansu Wind Farm, into the grid. His major interests lie in parallel computing for power system analysis, and big-data intelligence for the future smart grid.

Santiago Grijalva received M.Sc. and Ph.D. degrees in Electrical and Computer Engineering from the University of Illinois at Urbana-Champaign in 1999 and 2002, respectively.

He is Georgia Power Distinguished Professor of Electrical and Computer Engineering and Director of the Advanced Computational Electricity Systems (ACES) Laboratory at The Georgia Institute of Technology. His research interest is on decentralized power system control, power system informatics and economics, and future sustainable energy systems. He is the principal investigator for various research projects under Department of Energy, ARPA-E, EPRI, PSERC and other several industry and Government sponsors. From 2002 to 2009 he was with PowerWorld Corporation as a software architect and consultant. From 2013 to 2014 he was on assignment to the National Renewable Energy Laboratory (NREL) as founding Director of the Power System Engineering Center (PSEC).